

SUPPORTING INFORMATION

## **Reannotation of fly amanita L-DOPA dioxygenase gene enables its cloning and heterologous expression**

Douglas M. M. Soares,<sup>a,b</sup> Letícia C. P. Gonçalves,<sup>a</sup> Caroline O. Machado,<sup>a</sup> Larissa C. Esteves,<sup>a</sup> Cassius V. Stevani,<sup>a</sup> Carla C. Oliveira,<sup>b</sup> Felipe A. Dörr,<sup>c</sup> Ernani Pinto,<sup>c,d</sup> Flávia M. M. Adachi,<sup>b</sup> Carlos T. Hotta,<sup>b,\*</sup> and Erick L. Bastos<sup>a,\*</sup>

<sup>a</sup> Departamento de Química Fundamental, Instituto de Química, Universidade de São Paulo, 05508-000 São Paulo, SP, Brazil

<sup>b</sup> Departamento de Bioquímica, Instituto de Química, Universidade de São Paulo, 05508-000 São Paulo, SP, Brazil

<sup>c</sup> Departamento de Análises Clínicas e Toxicológicas, Faculdade de Ciências Farmacêuticas, Universidade de São Paulo, 05508-000 São Paulo, SP, Brazil

<sup>d</sup> Centro de Energia Nuclear na Agricultura, Universidade de São Paulo, 13400-970 Piracicaba, SP, Brazil

\* Corresponding authors: [hotta@iq.usp.br](mailto:hotta@iq.usp.br) (CTH), [elbastos@iq.usp.br](mailto:elbastos@iq.usp.br) (ELB)

## Contents

Material and methods .....	S3
General .....	S3
Buffers .....	S3
Standard compounds .....	S3
Apoenzyme preparation .....	S4
Kinetic modelling .....	S4
Figures .....	S6
Tables .....	S15
References .....	S16

## MATERIAL AND METHODS

### General

All chemicals were purchased from Sigma-Aldrich, and used without further purification, unless otherwise stated. Solutions were prepared using deionized water (18.2 M $\Omega$  cm at 25 °C, TOC  $\leq$  4 ppb, Milli-Q, Millipore). All values are expressed as the mean  $\pm$  standard deviation (SD) of three independent replicates.

### Buffers

**Sodium phosphate buffer** (50 mM, pH 7.4) was prepared by dissolving the appropriate amount of phosphate sodium salt in water, and adjusting the pH to 7.4, with NaOH at 25 °C.

**Sodium phosphate lysis buffer** (50 mM, pH 7.4, 0.3 M NaCl) was prepared by supplementing the sodium phosphate buffer with imidazole (10 mM), phenylmethanesulfonyl fluoride (PMSF, 1 mM),  $\beta$ -mercaptoethanol (2 mM), and one tablet of cOmplete protease inhibitor cocktail (Roche).

**Elution buffer** was prepared by supplementing the sodium phosphate lysis buffer with a linear gradient of imidazole from 100 mM to 500 mM.

### Standard compounds

**Betalamic acid (HBt)** was obtained according to the procedure described by Schliemann et al.,<sup>1</sup> with a few modifications. Fresh beetroot juice (200 mL) was paper-filtered and subjected to alkaline hydrolysis using NH<sub>4</sub>OH (pH 11.4, 30 min, room temperature [rt]). Next, the solution was cooled in an ice bath, and the pH was adjusted to 3 by slow addition of concentrated HCl. HBt was extracted with ethyl acetate (50 mL, 2 $\times$ ), and subjected to chromatographic and spectrophotometric analyses.

**L-Dopaxanthin** was obtained as described by Schliemann et al.,<sup>1</sup> with minor modifications. HBt in ethyl acetate was obtained from hydrolyzed beetroot juice. The acid was partitioned into

water, and the residual organic solvent was evaporated under reduced pressure (80 mm Hg, 25 °C). L-DOPA (50 equiv.) was added to a solution of HBt (5 mL) in water at pH 10. Depletion of HBt, and concomitant appearance of L-dopaxanthin were monitored spectrophotometrically at 430 nm and 470 nm, respectively. After completion, HCl (*conc.*) was added slowly until a pH of 5 was reached. The product was purified by gel chromatography using Sephadex LH-20 as the stationary phase and water as the eluent. Final characterization was carried out using LC-HRMS.

### **Apoenzyme preparation**

Sodium phosphate buffer (50 mM, pH 8.5) was treated with Chelex-100 (50 mg mL<sup>-1</sup>) for 24 h, and filtered, and the pH was confirmed and adjusted when necessary (Ch-PB). Stock solutions of ascorbic acid (250 mM) and L-DOPA (5 mM) were prepared using Ch-PB. The stock solution of AmDODA in sodium phosphate buffer (1.12 mg mL<sup>-1</sup>, 50 μM, 10 μL) was diluted 100-fold using Ch-PB and Chelex-100 (50 mg). pH of the supernatant was measured prior to use. The mixture was incubated at 4 °C and 450 rpm using an orbital mixer, and aliquots were taken every 30 min until the activity of the enzyme treated with Ch-PB was lost (3.5 h). Activity of the enzyme prepared with Ch-PB was compared to that of the negative control. All solutions were prepared using sodium phosphate buffer and incubated under the same conditions.

### **Kinetic modelling**

To model the kinetics of 2,3-seco-DOPA, 4,5-seco-DOPA, betalamic acid, muscaflavin, L-dopaxanthin, and L-DOPA hygroaurin formation, the observed rate constants ( $k_{obs}$ ) for the formation and/or consumption of these intermediates and products were calculated by non-linear fitting of the chromatographic data to mono- or biexponential functions using Origin 2016 software (OriginLab). Next, a minimal kinetic model was used to investigate the conversion of 1.0 mM L-DOPA into L-dopaxanthin and L-DOPA hygroaurin using COPASI v.4.22.<sup>2</sup> For simplicity, all elementary reactions were defined as unimolecular and irreversible, and the values of  $k_{obs}$  were

used to develop the model, ensuring that the resulting kinetic profile was qualitatively similar to the experimental data. The maximum theoretical concentration of each intermediate and product was divided by the maximum experimental absorption measured by HPLC-PDA analysis. The resulting factor was used to calculate the relative concentration of each species based on the experimental absorption. Changes in the concentration of each species over time were fitted to different kinetic models, and the first-order rate constants were calculated using the evolution programming method.

## FIGURES

```

1          10          20          30          40          50          60          70
Consensus sequence for clone 1  GGAAGTAAAAGTCGTAACAAGGTTTCCTAGGTTGAACCTGCGGAAGGATCATTATTGAAAGAACCTCAGGCAGGGGG
AB015700.1                      GGAAGTAAAAGTCGTAACAAGGTTTCCTAGGTTGAACCTGCGGAAGGATCATTATTGAAAGAACCTCAGGCAGGGGG
Consensus sequence for clone 2  GGAAGTAAAAGTCGTAACAAGGTTTCCTAGGTTGAACCTGCGGAAGGATCATTATTGAAAGAACCTCAGGCAGGGGG
AB080779.1                      GGAAGTAAAAGTCGTAACAAGGTTTCCTAGGTTGAACCTGCGGAAGGATCATTATTGAAAGAACCTCAGGCAGGGGG

80          90          100         110         120         130         140         150
Consensus sequence for clone 1  AGATGGTTGTAGCTGGCCTCAGGGGCATGTGCACACTGTGTCTCTCTTGGCTTGTTCCTCCACTTGTGC
AB015700.1                      AGATGGTTGTAGCTGGCCTCAGGGGCATGTGCACACTGTGTCTCTCTTGGCTTGTTCCTCCACTTGTGC
Consensus sequence for clone 2  AGATGGTTGTAGCTGGCCTCAGGGGCATGTGCACACTGTGTCTCTCTTGGCTTGTTCCTCCACTTGTGC
AB080779.1                      AGATGGTTGTAGCTGGCCTCAGGGGCATGTGCACACTGTGTCTCTCTTGGCTTGTTCCTCCACTTGTGC

160         170         180         190         200         210         220         230
Consensus sequence for clone 1  ACTGCTTGTAGGCAGCCCTGGCATTGTTCCAGGCTGTCTATGATTTTATTTACATACATGAACAATTGTTGTACAGAAT
AB015700.1                      ACTGCTTGTAGGCAGCCCTGGCATTGTTCCAGGCTGTCTATGATTTTATTTACATACATGAACAATTGTTGTACAGAAT
Consensus sequence for clone 2  ACTGCTTGTAGGCAGCCCTGGCATTGTTCCAGGCTGTCTATGATTTTATTTACATACATGAACAATTGTTGTACAGAAT
AB080779.1                      ACTGCTTGTAGGCAGCCCTGGCATTGTTCCAGGCTGTCTATGATTTTATTTACATACATGAACAATTGTTGTACAGAAT

240         250         260         270         280         290         300         310
Consensus sequence for clone 1  GTGATAAA- AAATAGTAATAACAACCTTCAACAACCGGATCTCTTGGCTCTCGCATCGATGAAGAACGCAGCGAAATGCG
AB015700.1                      GTGATAAA- AAATAGTAATAACAACCTTCAACAACCGGATCTCTTGGCTCTCGCATCGATGAAGAACGCAGCGAAATGCG
Consensus sequence for clone 2  GTGATAAA- AAATAGTAATAACAACCTTCAACAACCGGATCTCTTGGCTCTCGCATCGATGAAGAACGCAGCGAAATGCG
AB080779.1                      GTGATAAA- AAATAGTAATAACAACCTTCAACAACCGGATCTCTTGGCTCTCGCATCGATGAAGAACGCAGCGAAATGCG

320         330         340         350         360         370         380         390
Consensus sequence for clone 1  ATAAGTAATGTGAATTCAGAAATTCAGTGAATCATCGAATCTTTGAAACGCATCTTGGCTCTCCCTTGGTATTCCGAGGAG
AB015700.1                      ATAAGTAATGTGAATTCAGAAATTCAGTGAATCATCGAATCTTTGAAACGCATCTTGGCTCTCCCTTGGTATTCCGAGGAG
Consensus sequence for clone 2  ATAAGTAATGTGAATTCAGAAATTCAGTGAATCATCGAATCTTTGAAACGCATCTTGGCTCTCCCTTGGTATTCCGAGGAG
AB080779.1                      ATAAGTAATGTGAATTCAGAAATTCAGTGAATCATCGAATCTTTGAAACGCATCTTGGCTCTCCCTTGGTATTCCGAGGAG

400         410         420         430         440         450         460
Consensus sequence for clone 1  CATGCCGTGTTGAGTGTCAATTAATCTGTCAAACATGCACCTTGAGTGTGTTTTGGATTGTGGGAGTGTCTGCTGGC
AB015700.1                      CATGCCGTGTTGAGTGTCAATTAATCTGTCAAACATGCACCTTGAGTGTGTTTTGGATTGTGGGAGTGTCTGCTGGC
Consensus sequence for clone 2  CATGCCGTGTTGAGTGTCAATTAATCTGTCAAACATGCACCTTGAGTGTGTTTTGGATTGTGGGAGTGTCTGCTGGC
AB080779.1                      CATGCCGTGTTGAGTGTCAATTAATCTGTCAAACATGCACCTTGAGTGTGTTTTGGATTGTGGGAGTGTCTGCTGGC

470         480         490         500         510         520         530         540
Consensus sequence for clone 1  TTTATGAGCCAGCTCTCCTGAAATACATTAGCTTTGGGGGGAGGTGCCAAGTCACTTCTGCCTTTCCATTGGTGTGA
AB015700.1                      TTTATGAGCCAGCTCTCCTGAAATACATTAGCTTTGGGGGGAGGTGCCAAGTCACTTCTGCCTTTCCATTGGTGTGA
Consensus sequence for clone 2  TTTATGAGCCAGCTCTCCTGAAATACATTAGCTTTGGGGGGAGGTGCCAAGTCACTTCTGCCTTTCCATTGGTGTGA
AB080779.1                      TTTATGAGCCAGCTCTCCTGAAATACATTAGCTTTGGGGGGAGGTGCCAAGTCACTTCTGCCTTTCCATTGGTGTGA

550         560         570         580         590         600         610         620
Consensus sequence for clone 1  TAGATGAATTAACCTTATCTACGCCAGGAAAGCAGGCTTCAGGTGATGCACTGTGATCTCTCTGCTCTCTAATTGAC
AB015700.1                      TAGATGAATTAACCTTATCTACGCCAGGAAAGCAGGCTTCAGGTGATGCACTGTGATCTCTCTGCTCTCTAATTGAC
Consensus sequence for clone 2  TAGATGAATTAACCTTATCTACGCCAGGAAAGCAGGCTTCAGGTGATGCACTGTGATCTCTCTGCTCTCTAATTGAC
AB080779.1                      TAGATGAATTAACCTTATCTACGCCAGGAAAGCAGGCTTCAGGTGATGCACTGTGATCTCTCTGCTCTCTAATTGAC

630         640         650         660         670         680         690         696
Consensus sequence for clone 1  ATTTGCTGATAACTTGACCTCAAATCAGGTAGGACTACCCGCTGAACCTTAAGCATATCAATAAGCGGAGGA
AB015700.1                      ATTTGCTGATAACTTGACCTCAAATCAGGTAGGACTACCCGCTGAACCTTAAGCATATCAATAAGCGGAGGA
Consensus sequence for clone 2  ATTTGCTGATAACTTGACCTCAAATCAGGTAGGACTACCCGCTGAACCTTAAGCATATCAATAAGCGGAGGA
AB080779.1                      ATTTGCTGATAACTTGACCTCAAATCAGGTAGGACTACCCGCTGAACCTTAAGCATATCAATAAGCGGAGGA

```

**Figure S1.** Multiple alignment between two consensus sequences obtained from the DNA sequencing of internal transcribed spacer elements (ITS1 and 2) of the nuclear rDNA cluster in the *A. muscaria* specimens collected in Brazil, and two *A. muscaria* ITS sequences deposited in the NCBI nucleotide database (GenBank AB015700.1 and AB080779.1).

```

1  acatgcgctt  cgctactcaa  atatatccat  tggtttcgcy  acacgctggt  tccgaaccca
61  gagagtctcg  cgactctctt  cagaaattct  cccaacttgc  gttccttcaa  caccctttg
121  gtgcccgcgg  cagaggactg  cgacagttag  ccatgacgga  ttctttcatt  cctctctgac
181  gactatccat  gcagaggcca  ggattctgga  ctatgctagt  cctatcccac  ctcatctcat
241  gaaccttctt  tctctacgcc  agatgtcctt  cgttgttctt  ctttcgccgg  gcagacgcac
301  gttggcgcag  tttcctcgag  tggcatggtt  cacgtttaca  gcataatcaa  gctttgattt
361  accttgacag  gaaccacttc  cagtccgact  tggcctacat  tgcacatca  tgccgcaacc
421  ttcttagact  cgatcttgct  ttctcccatt  ggacggcata  tgccgtttcc  tgtagacctc
481  ccgcctacag  tggaacatct  gggcatcttt  tgtactcagg  gtcagatcgc  caactaccag
541  acgttcttct  ctcgttttaga  taggatcgcg  tatggtgcca  agcttcggtg  tatacagttc
601  ttgggtaaac  ggacgtcaga  gatatatctg  acaagcattt  gcatcaatto  tgggtctggca
661  cgaggcgact  aagaggtagt  ggggtagat  tcatgaatca  tagaggggca  tgtatagcgt
721  agctaaggat  agcactggca  gttccacagt  tctatataat  ccgtgatacg  actctctcgt
781  tcccctcaca  tactaccatg  tccaccaagc  cagagactga  ccttcaaact  gtctctgaca
841  gcgaaatcaa  gtttgtctag  tttgtctcca  ctagcaaaaa  ctctgctgac  ttgtgtacag
901  ggaatggcac  tttcgtcagt  cgaccaagca  acgactaact  tatgtagctc  aaattgacct
961  tgcaactaat  agacatctac  tttcatcaga  acaacgccgc  agagcatcaa  gctgcgcttg
1021  agcttcgtga  cgcggttctg  aggctcagac  aagacggcgc  attcgtcgc  gttcccttgt
1081  tcccggttaa  catggacccc  atgggtcctc  atcctgtcgg  tcagtagtca  tcgcaatcac
1141  accaccagtc  cttgaacaag  tcccttgact  ctcaaggttc  ttatgagatc  tgggttcggt
1201  ctgaaacggt  cgcttcggtg  ttctcctact  tgtgcatgaa  cagagggaga  ttaagcatcc
1261  ttgtgcatcc  ttgacacgc  gaagaactca  gagacatga  aattcgtaat  gcctggatag
1321  gacctctttt  cccactcaat  ctgcgcaacc  taccgatcaa  gagtgatgag  atccctttgc
1381  aatatccaag  cctcagtatg  tcatctcacc  actctctggc  ggccctcagt  gacaaattgt
1441  tgcagagctt  gggactcat  cgacagcgca  taagatgtca  ttggaagaaa  ggcggaaatt
1501  aggcgacgat  atagaagcag  tgcttagggg  agagaaagag  gcggccagag  cgccccatcg
1561  agatgcatag  agctacattc  gattgtctat  attgctactg  acatagggta  atgttggaat
1621  tttctgccc

```

**Figure S2.** DNA sequence for *doda* (Hinz *et al.*, 1997; GenBank accession Y12886, NCBI). *doda* exons are highlighted in blue and the inferred 3'-AG splice site, altered to GA in *A. muscaria* specimens analyzed, is highlighted in yellow. The start codon for 558-bp CDS is shown in red.

```

MVPSFVVYSSWVNGRQRYIRQAFASILFYIIRDTTLSFPSHTTMSTKPETDLQTVLDSEIKEWHFHIYFHQNNAAEHQ
AALELRDAVLRRLRQDGAFVAVPLFRVNMDPMGPHVPGSYEIWVPSETFASVFSYLCMNRGRLSILVHPLTREELRDHE
IRNAWIGPSFPLNLANLPKISDEIPLQYPSLKLGYSSSTAHKMSLEERRKLGDDIEAVLRGEKEAARAPHRDA-

```

**Figure S3.** Amino acid sequence inferred for 228-aa AmDODA encoded by *doda* (full sequence)<sup>3</sup> and the 185-aa AmDODA fragment (highlighted).

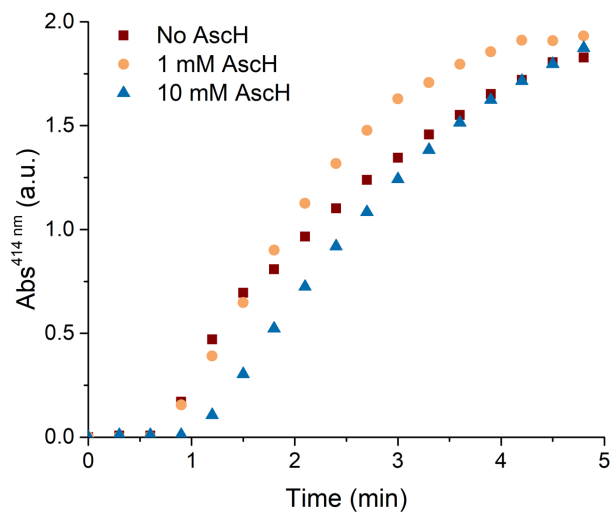


**Figure S4.** Effect of ascorbic acid (AscH) on the oxidative cleavage of L-DOPA catalyzed by AmDODA. Absorption at 414 nm of the conversion of L-DOPA (1 mM) by AmDODA (1  $\mu$ M) in the presence or absence of 1 or 10 mmol L<sup>-1</sup> AscH in sodium phosphate buffer (50 mM), pH 8.5.



**Figure S5.** Effect of the presence (left) or absence (right) of ascorbic acid (AscH) in the standard reaction without AmDODA. Picture credit: Dr. Douglas M. M. Soares.



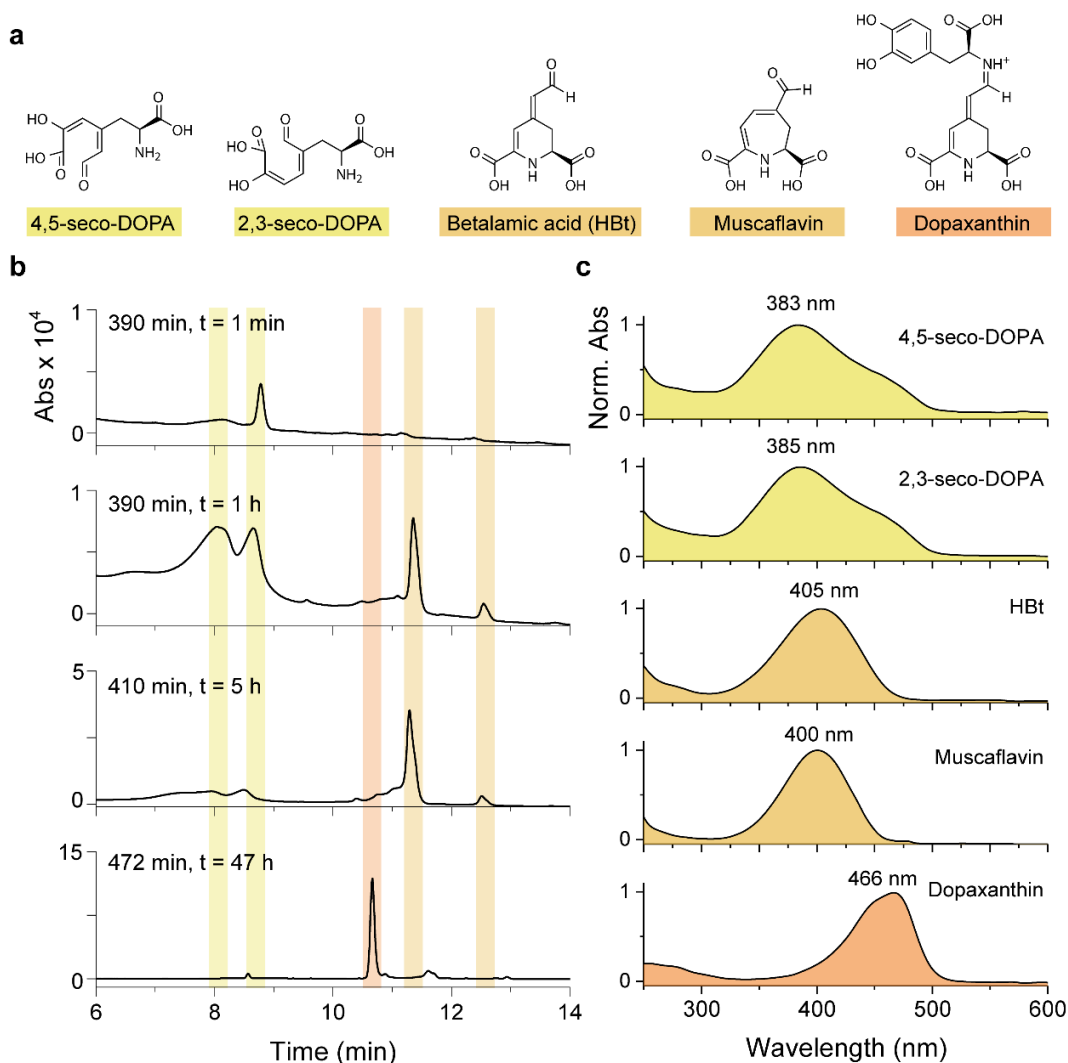


**Figure S6.** HPLC of 4,5-seco-DOPA and 2,3-seco-DOPA formed during oxidative cleavage of L-DOPA catalyzed by AmDODA, and the derived compounds (betalamic acid, muscaflavin and dopaxanthin). (a) Reaction products monitored by HPLC. (b) Chromatograms obtained at 390 nm (seco-DOPA), 410 nm (betalamic acid and muscaflavin), and 472 nm (dopaxanthin). Note that  $t$  corresponds to the time of injection after the reaction was triggered. (c) Spectra of the peaks of the reaction products with retention times: 8.1 min (383 nm, 4,5-seco-DOPA), 8.7 min (385 nm, 2,3-seco-DOPA), 10.7 min (466 nm, L-dopaxanthin), 11.3 min (405 nm, betalamic acid), 12.5 min (400 nm, muscaflavin). Reaction condition: [AmDODA] = 1  $\mu$ M, [AscH] = 10 mM, [L-DOPA] = 2.5 mM, sodium phosphate buffer (50 mM), pH 8.5.

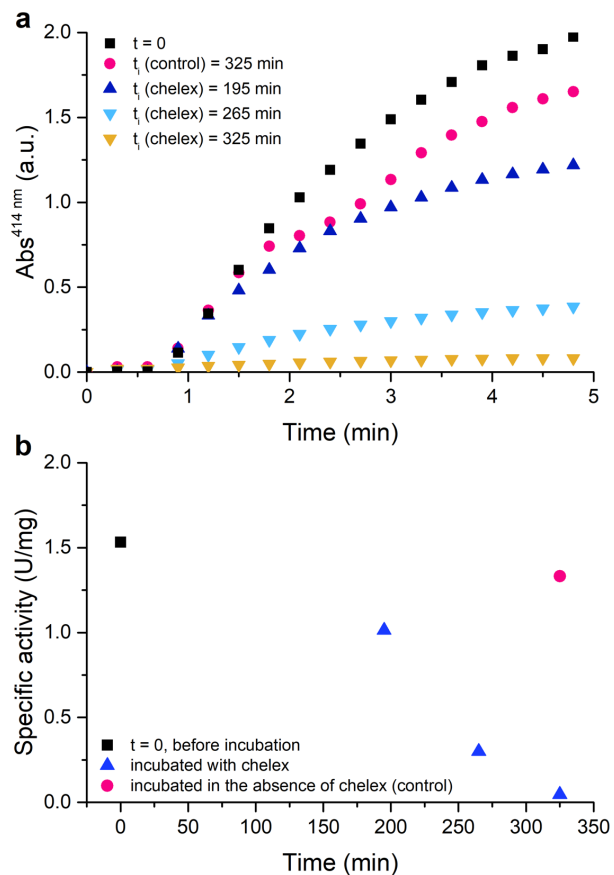


**Figure S7.** Effect of incubation with Chelex-100 on the oxidative cleavage of L-DOPA catalyzed by AmDODA. (a) Absorption at 414 nm for AmDODA (0.24 mg/mL) incubated at 4 °C under agitation (450 rpm), with or without Chelex-100, in sodium phosphate buffer (50 mM), pH 8.5. (b) Specific activity (U/mg) at the same conditions. Reaction condition: [AmDODA] = 1  $\mu$ M, [AsCH] = 10 mM, [L-DOPA] = 1 mM, sodium phosphate buffer (50 mM), pH 8.5.

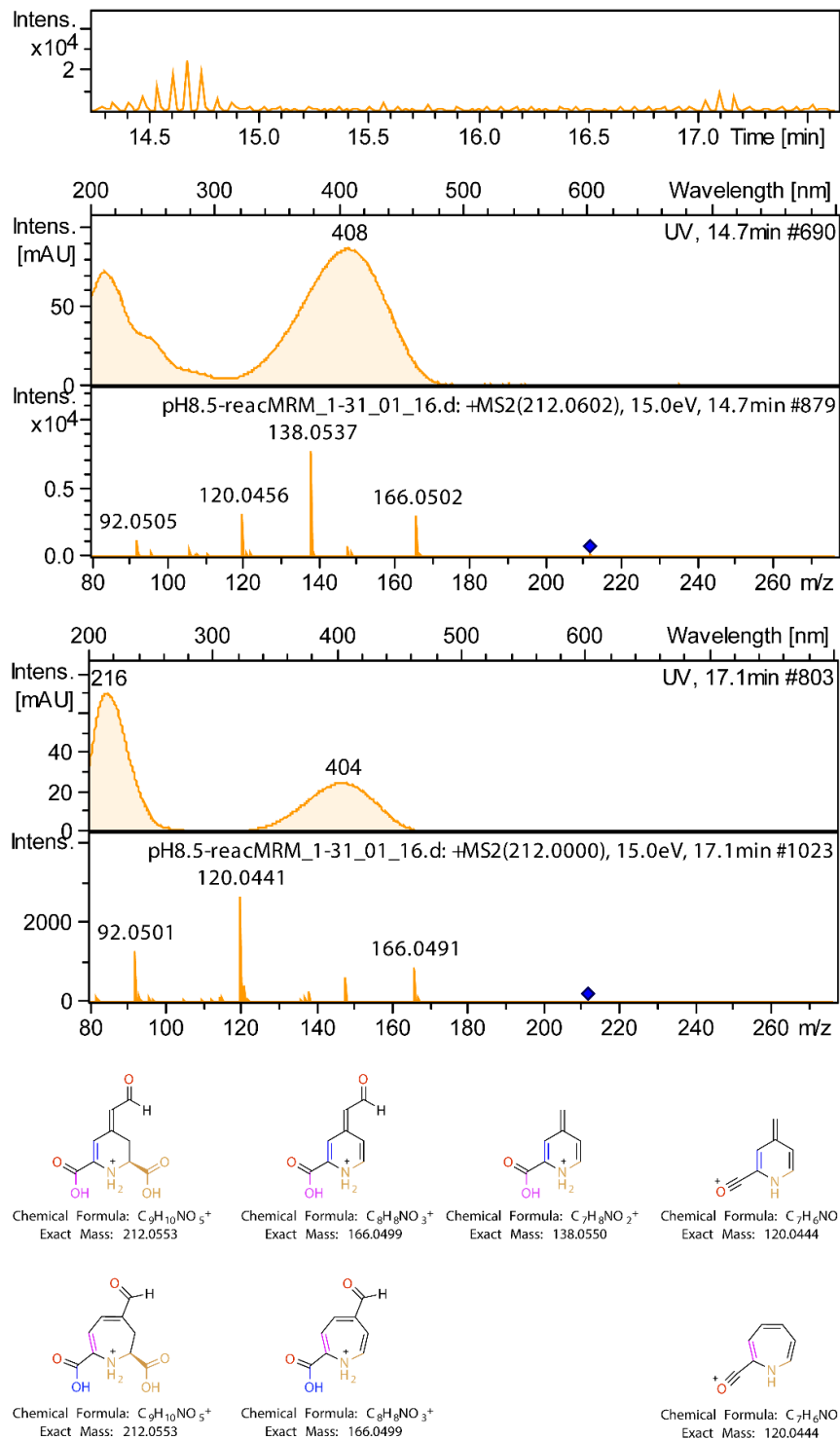


**Figure S8.** Comparison of HPLC-PDA-MS(EESI) and MS/MS analysis of the substances with retention time of 14.7 min and 17.1 min, which were characterized as betalamic acid and muscaflavin.

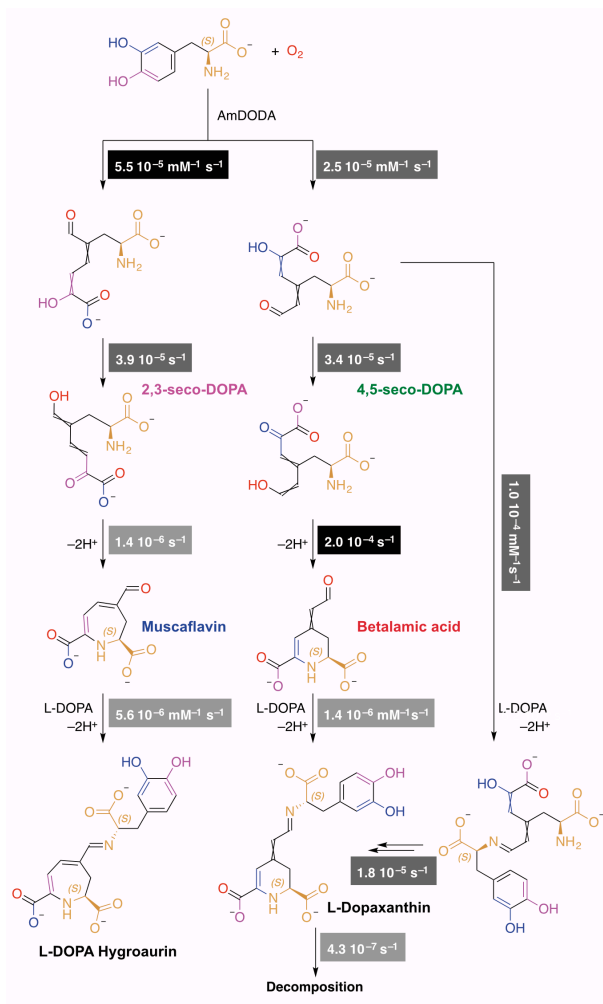


**Figure S9.** Kinetic modelling for the oxidative cleavage of L-DOPA by oxygen in the presence of AmDODA.

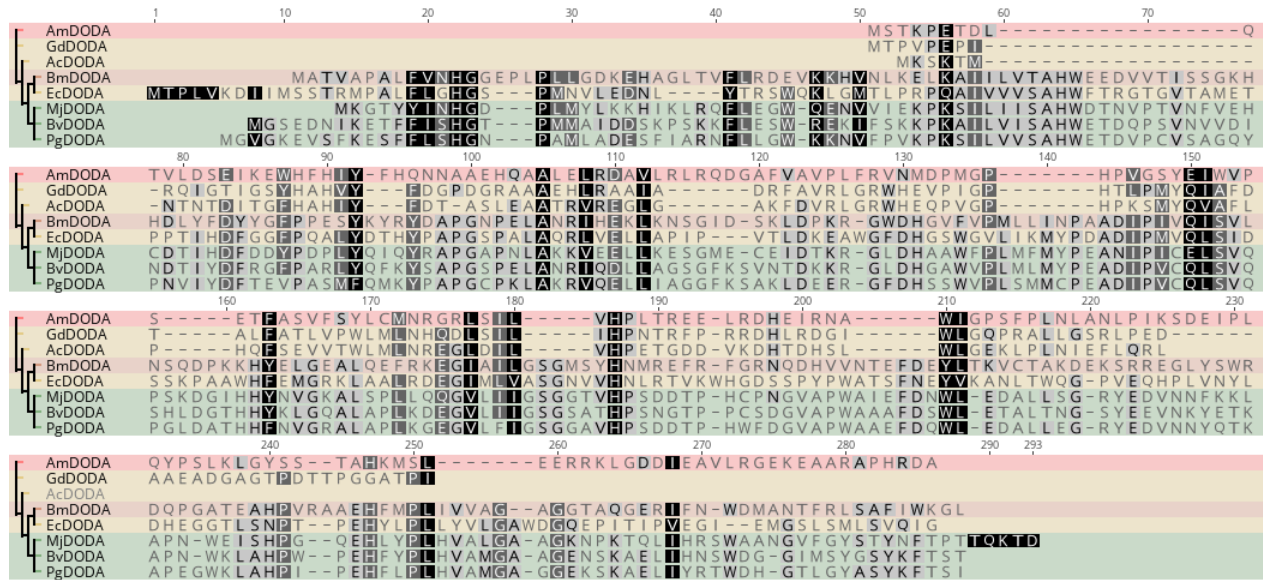


**Figure S10.** Multiple alignment of amino acid sequences of functionally characterized DODAs from fungi (*A. muscaria* – AmDODA), bacteria (*Gluconacetobacter diazotrophicus* – GdDODA, *Anabaena cylindrica* – AcDODA, *Escherichia coli* - EcDODA), insect (*Bombyx mori* – BmDODA) and plants (*Mirabilis jalapa* – MjDODA, *Beta vulgaris* – BvDODA and *Portulaca grandiflora* – PgDODA). Similarity of residues is indicated by colors: black for 100%, dark gray for 80-100%, and light gray for 60-80%. Not highlighted residues are less than 60% similar. The horizontal colors group sequences together according to similarity.

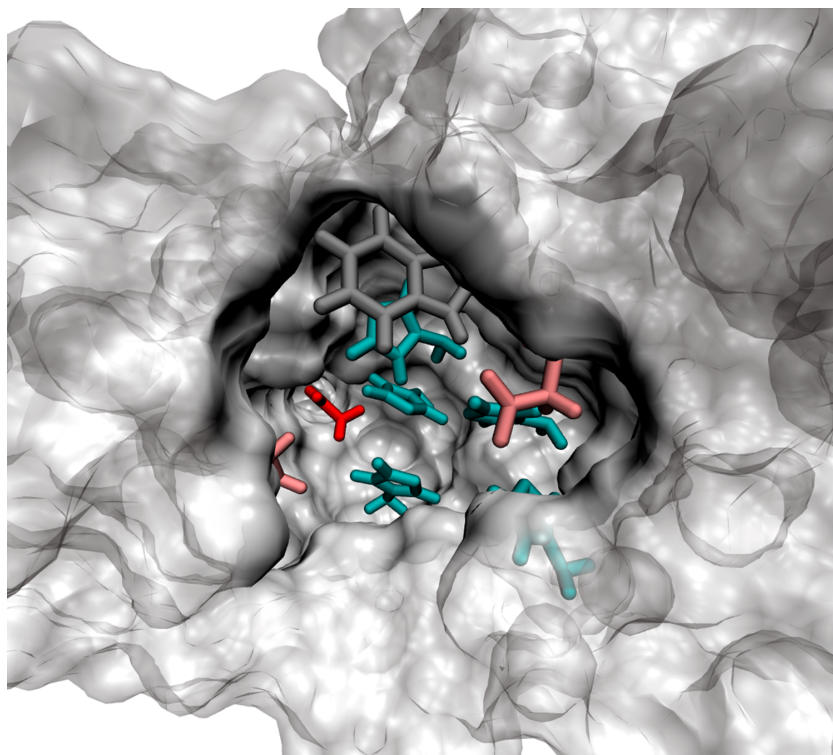


**Figure S11.** Catalytic pocket and amino acid residues located at regions I and II of AmDODA.

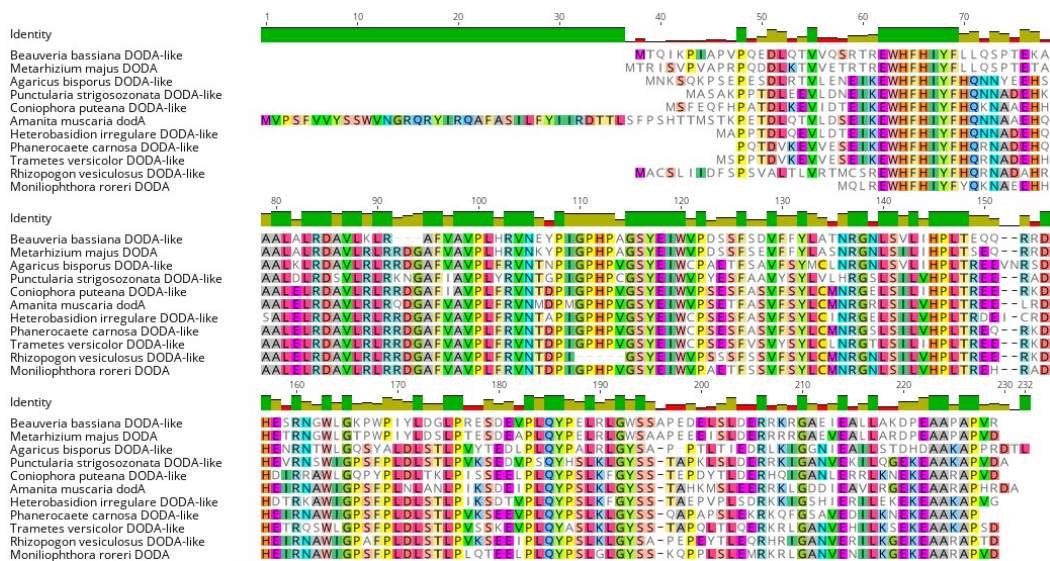


**Figure S12.** Multiple alignment of amino acid sequences of fungal L-DOPA-dioxygenases (MUSCLE, Geneious Prime v11.0.4).

## TABLES

**Table S1.** Alignments showing the main-chain root-mean-square deviation (RMSD, in Å) below the diagonal, and the number of overlapping residues above the diagonal.

<b>Protein</b>	<b>1</b>	<b>2</b>	<b>3</b>	<b>4</b>
AmDODA_Hinz <i>et al.</i> (1)		121	99	106
AmDODA (2)	0.504		99	106
AcDODA (3)	1.010	0.994		99
GdDODA (4)	0.875	0.853	0.744	

**Table S2.** Homology models used for the metal cation binding sites of DODAs.

<b>Rank</b>	<b>Template</b>	<b>Confidence</b>	<b>Coverage</b>	<b>Seq. id.</b>	<b>E-value</b>	<b>z-score</b>
<b>AmDODA</b> , TM-score = 0.667						
1	2P8I_D	100	62.2	40.0	4.9E-51	85.540
2	2PEB_A	100	61.1	39.8	5.8E-50	82.898
<b>GdDODA</b> , TM-score = 0.790						
1	2P8I_D	100	79.6	45.2	9.7E-50	87.542
2	2PEB_A	100	79.6	43.4	2.2E-50	87.532
<b>AcDODA</b> , TM-score = 0.907						
1	2PEB_A	100	94.1	69.9	2.2E-51	84.713
2	2P8I_D	100	95.0	45.2	9.9E-51	82.726

## REFERENCES

1. Schliemann, W.; Kobayashi, N.; Strack, D., The decisive step in betaxanthin biosynthesis is a spontaneous reaction. *Plant Physiol* **1999**, *119* (4), 1217-1232.
2. Hoops, S.; Sahle, S.; Gauges, R.; Lee, C.; Pahle, J.; Simus, N.; Singhal, M.; Xu, L.; Mendes, P.; Kummer, U., COPASI—a COmplex PAthway SIMulator. *Bioinformatics* **2006**, *22* (24), 3067-3074.
3. Hinz, U. G.; Fivaz, J.; Girod, P. A.; Zrýd, J. P., The gene coding for the DOPA dioxygenase involved in betalain biosynthesis in *Amanita muscaria* and its regulation. *Mol Gen Genet* **1997**, *256* (1), 1-6.